Image Rendering of Art Paintings

Total Archives Considering Surface Properties and Chromatic Adaptation

Shoji Tominaga, Mariko Nakagawa and Norihiro Tanaka
Department of Engineering Informatics, Osaka Electro-Communication University
Neyagawa, Osaka, Japan

Abstract

This paper describes an image rendering method for total digital archives of art paintings on a display device by considering surface properties and chromatic adaptation. First, we estimate the surface properties, including surface normal, surface-spectral reflectance, and reflection model parameters. We use a multi-band camera with six spectral channels. Multiple images of a painting are acquired with different illumination directions. All the estimated surface data are combined for image rendering. Next, we develop a chromatic adaptation transform for predicting appearance of the paintings under the illumination of an incandescent lamp and producing the full color images on a monitor. An incomplete adaptation index representing the degree of chromatic adaptation is defined based on color temperatures. The experimental results suggest the feasibility of the proposed.

Introduction

Practical digital archiving of art paintings including oil paintings is based on both shape information for describing surface geometries and spectral information for color reproduction. A direct way to acquire the shape data of object surfaces is to use a laser rangefinder.[1] This device, however, make unavoidable errors in measuring colored paintings that include specularity, which differ from white matte surfaces. The authors[2] showed that the surface shape of a painting was represented by a set of surface normal vectors of small facets that were estimated from camera data. Next, the spectral reflectance information is more useful than color information.[3,4] In fact, an RGB image is device-dependent and valid for only the fixed conditions of illumination and viewing. The surface normals and surface spectral reflectances are estimated from camera data, and the estimates are used for rendering realistic images of the paintings under arbitrary conditions.

We should note the viewing conditions for art paintings. Most art paintings are hung on the wall indoors, which are often illuminated with incandescent lamps. In this situation, we cannot neglect the effect of chromatic adaptation that is the most important color-appearance phenomenon of the human visual system.

The present paper describes an image rendering method for total digital archives of art paintings on a display device by considering surface properties and chromatic adaptation. In the process of the total digital archives, we estimate precisely the surface properties, including surface normal, surface spectral reflectance, and reflection model parameters. Here we use a multi-band camera with six spectral channels. Multiple images of a painting are acquired with different illumination directions. All the estimated surface data are combined for image rendering.

There are many kinds of chromatic-adaptation and color-appearance models (e.g., see Refs. [5]-[7]). Most of the models were developed based on experimental data using color patches. These models consist of complicated equations with many parameters. We have to specify precisely the viewing conditions on luminance, background, and surround. Therefore, the previous models are difficult to apply to the problem of image rendering of art paintings in the present study.

In this paper, a chromatic adaptation transform is developed for predicting appearance of the paintings under the illumination of an incandescent lamp and producing the full color images on a monitor. We extend the von Kries' framework to incomplete chromatic adaptation. An incomplete adaptation index representing the degree of chromatic adaptation is defined based on color temperatures of the Blackbody radiators. This index is determined numerically by the visual experiment of memory matching between real paintings and the images displayed on a monitor.

Measuring System

The multi-band camera system is composed of a monochrome CCD camera, a standard photographic lens, six color filters, and a personal computer. Figure 1 shows the composite spectral sensitivity functions for six sensors. The image acquisition of the same object surface is repeated for different illumination directions. The camera aims at the object surface from vertically above the painting. The position of a light source is changed around the optical axis (Z axis). In practice, multi-band images are captured under 16 illumination directions, except for the extreme raking lights. The light source for measuring surface properties is a slide projector lamp.

The multiple illuminations have two advantages. First, the most reliable function of spectral reflectance without specularity and shadowing effects is selected from the image set observed under different directions. Second, the surface normal vector is estimated from the change in shading as the illumination direction changes.

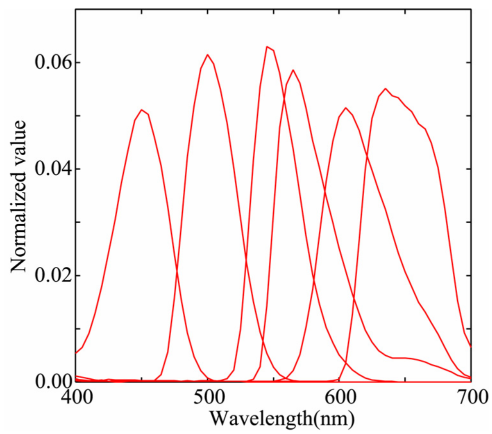

Figure 1. Spectral-sensitivities of the camera.

Surface Reflection Model

We use the Torrance- Sparrow model[8] as a reflection model for the surface of a painting. In this mode, the spectral radiance $Y(\lambda)$ from a reflective surface is described as

$$Y(\lambda) = (\mathbf{N}\cdot\mathbf{L})S(\lambda)E(\lambda) + \beta\frac{D(\varphi,\gamma)F(\theta_Q)G(\mathbf{N},\mathbf{V},\mathbf{L})}{\mathbf{N}\cdot\mathbf{V}}E(\lambda), \quad (1)$$

where the first and second terms represent, respectively, the diffuse and specular reflection components. Vectors **N**, **V**, and **L** represent the global surface normal vector, the view vector, and the illumination directional vector. **Q** is the bisector vector of **L** and **V**. φ is the angle between **N** and **Q**. $S(\lambda)$ is the surface-spectral reflectance, and $E(\lambda)$ is the illuminant spectrum.

The specular component in Eq.(1) consists of three terms: D is a function providing the index of surface roughness defined as $\exp\{-\ln(2)\varphi^2/\gamma^2\}$. G is a geometrical attenuation factor. F represents the Fresnel reflectance, where θ_Q is the incidence angle to a micro-facet. This reflectance depends on the index of refraction, n. We assume n=1.45 as the average of dielectric materials. β represents the intensity of the specular component.

The parameters **N**, $S(\lambda)$, γ, and β are estimated below.

Estimation of Surface Properties

The sensor output for a painting surface is composed of two additive components, the diffuse reflection and the specular reflection. The spectral reflectance function and the surface normal are then estimated from the diffuse reflection component. The specular reflection parameters are estimated from the specular reflection component. We devised a procedure to detect the diffuse reflection component at each pixel point of the multiple images acquired under different illumination directions.

Surface Normal

We use a photometric stereo method[9] to compute the surface normal vector at each pixel of an observed art painting. If an object surface is a perfect diffuser (Lambertian), the light intensity (radiance) I reflected from the surface illuminated by a light source is described as $I = \alpha\mathbf{N}^t\mathbf{l}_i$, where $\mathbf{l}_i$ is the illumination directional vector of i-th light source, and α is the diffuse reflectance factor. Therefore the problem of estimating the three-dimensional vector **N** can be solved using radiance values at more than three different illumination directions.

Spectral Reflectance

The sensor outputs for a diffuse object are described as

$$\rho_k = \int_{400}^{700} S(\lambda)E(\lambda)R_k(\lambda)d\lambda + n_k, \ (k = 1, 2, \ldots, 6), \quad (2)$$

where $R_k(\lambda)$ is the spectral sensitivities of the k-th sensor, and n_k is noise. The discrete form is expressed as

$$\rho_k = \sum_i S(\lambda_i)E(\lambda_i)R_k(\lambda_i)\Delta\lambda + n_k, \ (k = 1, 2, \ldots, 6). \quad (3)$$

Next, let $\boldsymbol{\rho}$ be a six-dimensional column vector representing the camera outputs, and **s** be a n-dimensional vector representing the spectral reflectance $S(\lambda)$. Moreover, define a 6xn matrix $\mathbf{H}\,(\equiv[h_{ki}])$ with the element $h_{ki} = E(\lambda_i)R_k(\lambda_i)\Delta\lambda$. Then the above imaging relationships are summarized in the matrix form

$$\boldsymbol{\rho} = \mathbf{H}\,\mathbf{s} + \mathbf{n}. \quad (4)$$

The solution method minimizing the estimation error on **s** has been studied in the linear system theory. When the signal component **s** and the noise component **n** are uncorrelated, the Wiener estimator gives an optimal solution as

$$\hat{\mathbf{s}} = \mathbf{R}_{ss}\mathbf{H}^t\left[\mathbf{H}\mathbf{R}_{ss}\mathbf{H}^t + \sigma^2\mathbf{I}\right]^{-1}\boldsymbol{\rho}, \quad (5)$$

where $\mathbf{R}_{ss}$ is an nxn matrix representing a correlation among surface spectral reflectances. A database of surface-spectral reflectances for about 500 different objects was used for making the correlation matrix. The database consists of one set of 354 reflectances made by Vrhel et al.[10] and another set of 153 reflectances that we measured from different paint samples. We assume white noise with a correlation matrix $\sigma^2\mathbf{I}$.

Model Parameters

The sensor output with the maximal intensity among the set of sensor outputs for different illumination directions has the possibility of including the specular reflection component. To detect the specular component, we first calculate the output vector $\boldsymbol{\rho}_{\mathrm{D}}$ for the diffuse component by using the estimated reflectance $\hat{S}(\lambda)$. Next, select the maximal sensor output $\boldsymbol{\rho}_{\mathrm{M}}$ among all observations, and define the difference $\boldsymbol{\rho}_{\mathrm{S}} = \boldsymbol{\rho}_{\mathrm{M}} - \boldsymbol{\rho}_{\mathrm{D}}$.

The specular function of the Torrance-Sparrow model is fitted to the specular data extracted from the entire pixel points. Since the specular component at any pixel has the same spectrum as the light source, the parameters are estimated based on the statistical distribution of the specular component. Define the intensity of the specular component as $\|\boldsymbol{\rho}_{\mathrm{s}}\|$, and normalize the specular component as $\rho_{\mathrm{s}} = \|\boldsymbol{\rho}_{\mathrm{s}}\| (\cos(\theta_{\mathrm{i}})\cos(\theta_{\mathrm{r}})) / (G(\mathbf{n},\mathbf{v},\mathbf{l})F(\theta_{\mathrm{Q}}))$.

Then, minimize the squared sum of the fitting error

$$e = \sum_x \left\{ \rho_{\mathrm{S}x} - \beta D(\varphi_x, \gamma) \right\}^2, \qquad (6)$$

where $\rho_{\mathrm{S}x}$ and φ_x are the specular intensity and angle at different pixel point x. Figure 2 shows an example of the intensity distribution as a function of angle φ. The vertical axis indicates ρ_{s}, and red dots indicate the observations. γ and β minimizing the error are solved as a solution of the nonlinear fitting problem. We use the Levenberg-Marquardt method for this solution.

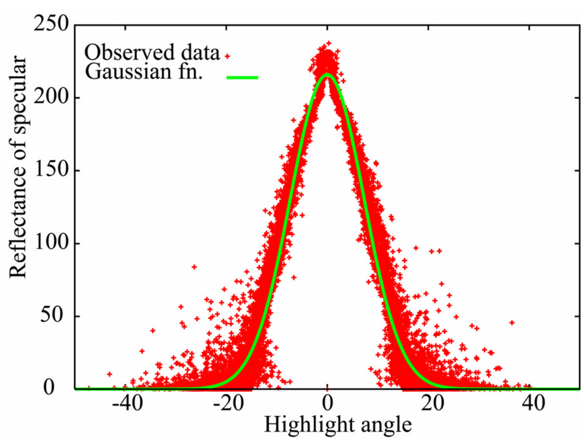

Figure 2. Distribution of the specular component.

Image Rendering

Colorimetric Rendering Algorithm

Computer graphics images of the target oil painting are created using the estimated surface normals and spectral reflectances at all pixel points, and the above determined the Torrance- Sparrow reflection model in Eq.(1). A ray-casting algorithm is adopted for the image rendering under parallel rays from the light source.

For the purpose of accurate color image rendering, the color images of art paintings are not represented by RGB values, but represented by the CIE tristimulus values XYZ. We calculate the XYZ values at each pixel by using the spectral radiance *Y (λ)* and the CIE standard color-matching functions.

The present study uses a CRT color monitor as the display device. First of all we have to adjust the color range of an image to the dynamic range of the monitor. Let Y_W and $Y_{\max}$ be, respectively, the maximum Y value in an image and the maximum luminance in the monitor white at (R, G, B)=(255, 255, 255). The data transformation for $Y_W = Y_{\max}$ is necessary. The standard monitor calibration consists of two steps of (1) color coordinate transformation and (2) Gamma correction. First, we transform the tristimulus values into the monitor RGB values by a transformation matrix, and second correct the RGB values into the practical RGB digital values by a lookup table.

Prediction of Incomplete Chromatic Adaptation

A. Model

We propose a color prediction method for incomplete chromatic adaptation that is based on an extended version of the von Kries model using correlated color temperature scale. We use Illuminant D65 as reference and Illuminant A as test in the present study. The adaptation process is considered incomplete adaptation along the color temperature scale. Then, an incomplete adaptation index $0 \le d \le 1$, representing the degree of chromatic adaptation, is introduced on the color temperature scale between the test illuminant A and the reference illuminant D65.

Figure 3 illustrates the incomplete adaptation process used. Because the color temperature scale (in kelvin K) is not correlated to perceived color differences, the present study uses a *reciprocal megakelvin* temperature scale. The unit of this scale is the reciprocal megakelvin (MK^{-1}), and a given small interval in this scale is approximately perceptible. Let $[MK^{-1}]_{\mathrm{T}}$ and $[MK^{-1}]_{\mathrm{R}}$ be the reciprocal temperatures of the test illuminant and the reference illuminant, respectively. Then, the color temperature of adaptation illumination corresponding to the index *d* is determined as

$$T_{\mathrm{D}} = 10^6 / (([MK^{-1}]_{\mathrm{R}} - [MK^{-1}]_{\mathrm{T}})d + [MK^{-1}]_{\mathrm{T}}). \qquad (7)$$

The spectral power distribution corresponding to T_{D} is given by the formula [13]

$$E(\lambda) = \mathrm{c}_1\ \lambda^{-5}\ \{\exp(\mathrm{c}_2/\lambda T_{\mathrm{D}}) - 1\}^{-1}, \qquad (8)$$

where $\mathrm{c}_1 = 3.7418 \times 10^{-16}$ Watts-m^2 and $\mathrm{c}_2 = 1.4388 \times 10^{-2}$ Watts-K and λ is wavelength (m). This distribution is used for only calculation of the pixel values of images.

A proper value of the incomplete adaptation index *d* is determined on matching experiments between real paintings under Illuminant A and the images on the monitor.

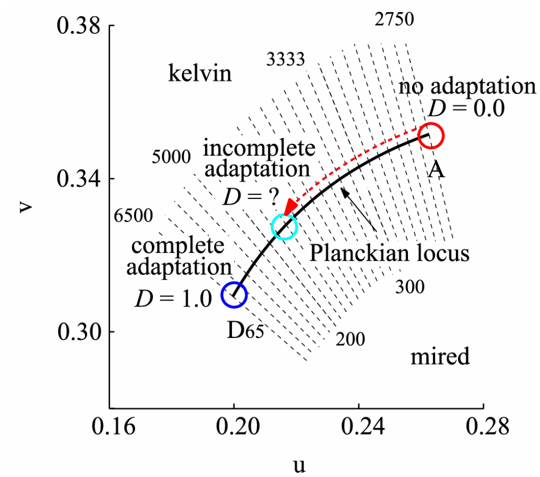

Figure 3. Incomplete adaptation process.

B. Color Transformation of Images

The image of an art painting under a specified illuminant condition is represented as an array of the tristimulus values XYZ. The color values of each pixel are then transformed by taking the chromatic adaptation effect into account. We use a von Kries-type transformation.

First, all XYZ values are transformed to relative cone responses (LMS) using a linear matrix multiplication[6]

$$\begin{bmatrix} L \\ M \\ S \end{bmatrix} = \mathbf{M} \begin{bmatrix} X \\ Y \\ Z \end{bmatrix}, \tag{9}$$

where

$$\mathbf{M} = \begin{bmatrix} 0.40024 & 0.70760 & -0.08081 \\ -0.22630 & 1.16532 & 0.04570 \\ 0 & 0 & 0.91822 \end{bmatrix}.$$

Second, let us define gain coefficients w_L, w_M, and w_S for modeling chromatic adaptation in which each of the three cone types has a separate gain coefficient. The gain coefficients are calculated as the ratio of the cone responses for white under the adaptation illuminant to the responses under the test illuminant as

$$w_L = L_D / L_T, \quad w_M = M_D / M_T, \quad w_S = S_D / S_T. \tag{10}$$

The symbol D represents the illuminant corresponding to the incomplete adaptation index *d*.

Then, the cone signals corresponding to the pixel value of an image under incomplete adaptation illuminant D are described as

$$\begin{bmatrix} L_p(D) \\ M_p(D) \\ S_p(D) \end{bmatrix} = \mathbf{W} \begin{bmatrix} L \\ M \\ S \end{bmatrix}, \tag{11}$$

where

$$\mathbf{W} = \begin{bmatrix} w_L & 0 & 0 \\ 0 & w_M & 0 \\ 0 & 0 & w_S \end{bmatrix}$$

The above equation represents a simple model of chromatic adaptation with separate gain coefficients.

Calculation in Eq. (11) is executed to all pixels of the original image under the test illuminant. Finally, the LMS image is inversely transformed into the XYZ image. The entire process of color transformation is summarized as

$$\begin{bmatrix} X_p(D) \\ Y_p(D) \\ Z_p(D) \end{bmatrix} = \mathbf{M}^{-1}\mathbf{W}\mathbf{M} \begin{bmatrix} X \\ Y \\ Z \end{bmatrix}. \tag{12}$$

Note that, when *d* is equal to 1.0, this process reduces to the basic algorithm for complete chromatic adaptation.

Experiments

Accuracy of the Estimated Surface Properties

Figure 4 shows the oil painting of a natural scene. First, surface normals were estimated at all pixel points of the painting. To investigate the accuracy, we compared the estimation results with the direct measurements to a small area in the red rectangular area of Figure 4. Figure 5 depicts the needle maps of the surface normals for the two cases. The estimated normals by the proposed method approximate measurements by the laser microscope closely.

Next, the estimation accuracy of surface-spectral reflectances was examined at 24 areas as shown by white rectangles in Figure 5. The estimated reflectances were then compared with the direct measurements and also with the estimates by the previous method.[2] Figure 6 shows the comparisons for Area 1 and Area 2, where the red curves, the dashed curves, and the dotted-dashed curves represent, respectively, the estimates by the proposed method, direct measurements, and the estimates by the previous method. The proposed method recovers the detailed shape of spectral reflectance accurately.

Third, the parameters of the 3D reflection model were estimated. Figure 3 shows the intensity distribution of the specular component in the read rectangular area. The Gaussian function was fitted to those specular data. Then the estimates were obtained as $\gamma = 197$ and $\beta = 0.14$.

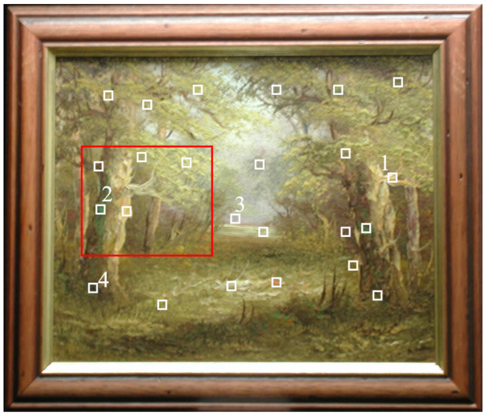

Figure 4. Oil painting of a natural scene.

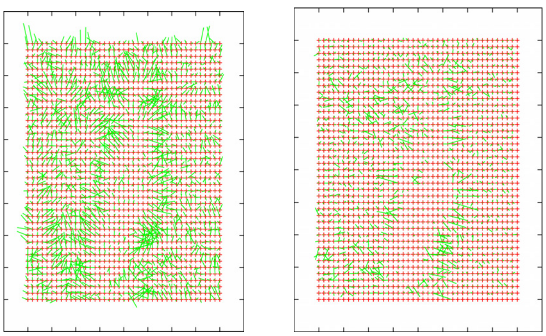

Figure 5. Needle maps of the estimated surface normals for the proposed method (left) and a laser microscope (right).

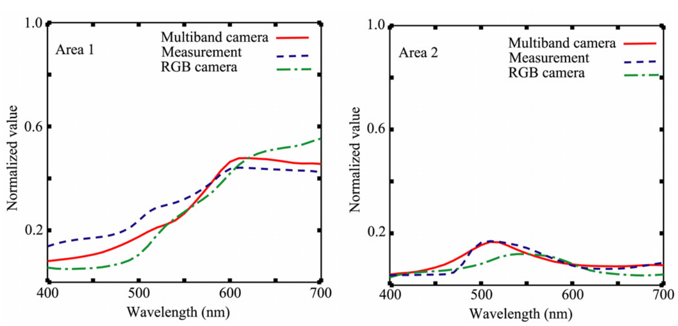

Figure 6. Estimated surface-spectral reflectances for Areas 1 –2.

Adaptation Experiment

Conditions

Figure 7 shows our experimental setup for predicting incomplete chromatic adaptation to art paintings. A calibrated CRT monitor and a target painting are placed on a table in a dark room. The test light is a diffuse light source of Illuminant A using an incandescent lamp and a diffuse filter. White on the monitor and white under the illuminant have the same luminance of about 60cd/m^2.

The experiments were conducted by using the method of memory matching between the target object and the images on the monitor. In the memory matching, subjects observe the target object for the adaptation time of three minutes and generate a match to the remembered image of the object in the second viewing condition. The adaptation index *d* can take intermediate values between 0.0 and 1.0 for various degrees of incomplete chromatic adaptation. We created computer graphics images corresponding to several *d* values. The subjects were instructed to select the displayed image that was the most closer in color appearance to the remembered original painting. The displayed image on the monitor is changed in random order of the *d* value by a simple keyboard operation.

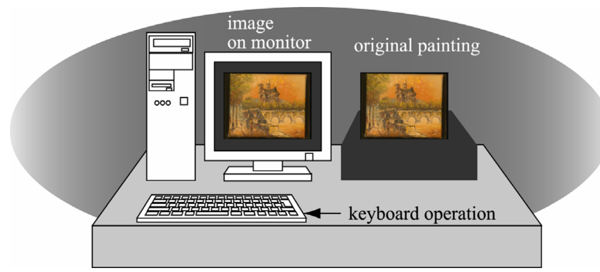

Figure 7. Setup for incomplete color adaptation.

Results

Two oil paintings, one of which is in Figure 4, were used in this experiment. The computer graphics images were created using the estimates of surface normal and surface-spectral reflectance under Illuminant A. We set up the viewing condition without strong specular reflection from the painting surface. We evaluated not only the proposed method but also the other methods including the Nayatani model in the image adaptation experiment

Fourteen subjects joined the evaluation. The proposed method and the Nayatani method were properly selected. We can see that there is no particular difference in the selection between the two paintings. The results suggest that the proposed method with $d = 0.5$ - 0.7 provides the most proper prediction for the paintings. The averaged value of the adaptation index is $d = 0.56$.

Rendering Results

Computer graphics images of the target oil paintings were created using the estimated surface normals and spectral reflectances, and the 3D reflection model. A ray-casting algorithm was adopted for the image rendering under parallel rays from light sources. Figure 8 shows the image rendering results under Illuminant A (2862K) corresponding to incandescent lamps that were based on the colorimetric rendering without any chromatic adaptation effect. The left picture represents the image from the front viewpoint. The right picture represents the image from a slanting viewpoint, where the surface roughness and the gloss are observed.

The image rendering results with the incomplete chromatic adaptation effect are shown in Figure 9, where the original images under Illuminant A were transformed using the proposed algorithm with d = 0.56. The illuminant in d=0.56 corresponds to the Blackbody radiator with a color temperature of 240 mired (4170K). These experimental results suggest that the proposed image rendering method can create realistic 3D images of art paintings under arbitrary illumination and viewing conditions for the purpose of total digital archives considering various surface properties and incomplete chromatic adaptation.

Figure 8. Image rendering results without any chromatic adaptation under Illuminant A (left: front view, right: slant view)

Figure 9. Image rendering results with incomplete chromatic adaptation under Illuminant A. (left: front view, right: slant view)

Conclusion

This paper has described an image rendering method for total digital archives of art paintings on a display device by considering surface properties and chromatic adaptation. First, we estimated the surface properties, including surface normal, surface-spectral reflectance, and reflection model parameters. Multiple images of a painting by the six-channel camera were acquired with different illumination directions. All the estimated surface data were combined for image rendering. Next, we developed a chromatic adaptation transform for predicting appearance of the paintings. We extended the von Kries' framework to incomplete chromatic adaptation. The incomplete adaptation index was defined based on color temperatures. The experimental results suggested the feasibility of the proposed method for image rendering under arbitrary illumination and viewing conditions.

References

1. S. Tominaga and N. Tanaka: 3D Recording and Rendering of Art Paintings, Proc. Ninth Color Imaging Conf., pp.337-341, 2001.
2. N. Tanaka and S. Tominaga: Measuring and Rendering Art Paintings Using an RGB Camera, Proc. of EUROGRAPHICS, pp.299-306, 2002.
3. H. Maitre et al.: Spectrophotometric image analysis of fine art paintings, Proc. Fourth Color Imaging Conf., pp.50-53, 1996.
4. Y. Miyake, et al.: Development of multiband color imaging systems for recording of art paintings, Proc. SPIE: Color Imaging, Vol.3648, pp.218-225, 1999.
5. Y. Nayatani: A Simple Estimation Method for Effective Adaptation Coefficient, Color Res. Appl. Vol.22, pp.259-268, 1997.
6. M. D. Fairchild: Color Appearance Models, Addison-Wesley, 1998.
7. N. Moroney, M. D. Fairchild, R. W. G. Hunt, C. Li, M. R. Luo and T. Newman: The CIECAM02 Color Appearance Model, Proc. Tenth Color Imaging Conf., pp.23-27, 2002.
8. K. E. Torrance and E. M. Sparrow: Theory for off-specular reflection from roughened surfaces, J. of Optical Society of America A, Vol.57, No.9, pp.1105-1114, 1967.
9. K. Ikeuchi: Determining a depth map using dual photometric stereo, Int. J. of Robotics Research, Vol.6, pp.15-37, 1987.
10. M. J. Vrhel et al.: Measurement and analysis of object reflectance spectra, Color Res. and Appl., Vol.19, pp.4-9, 1994.
11. G. Wyszecki and W.S. Stiles: Color science: concepts and methods, quantitative data and formulae, Wiley, 1982.

Biography

Shoji Tominaga received the B.E., M.S., and Ph.D. degrees in electrical engineering from Osaka University, Toyonaka, Osaka, Japan, in 1970, 1972, and 1975, respectively. Since 1976, he has been with Osaka Electro-Communication University, Neyagawa, Osaka, where he is currently a Professor with the Department of Engineering Informatics, and a Dean of the Faculty of information Science and Arts. His research interests include computer graphics, color image analysis, reflection modeling, and color vision. He is a senior member of IEEE and a member of OSA, IS&T, SID, SPIE, and ACM.